Resonant two-photon ionization spectroscopy of jet-cooled OsN: 520–418 nm

Maria A. Garcia and Michael D. Morse[a)]

Department of Chemistry, University of Utah, Salt Lake City, Utah 84112, USA

(Received 18 July 2011; accepted 14 August 2011; published online 16 September 2011)

The optical transitions of supersonically cooled OsN have been investigated in the range from 19 200 to 23 900 cm^{-1} using resonant two-photon ionization spectroscopy. More than 20 vibronic bands were observed, 17 of which were rotationally resolved and analyzed. The ground state is confirmed to be $^2\Delta_{5/2}$, deriving from the $1\sigma^2\ 2\sigma^2\ 1\pi^4\ 1\delta^3\ 3\sigma^2$ electronic configuration. The X $^2\Delta_{5/2}$ ground state rotational constant for $^{192}Os^{14}N$ was found to be $B_0 = 0.491921(34)$ cm^{-1}, giving $r_0 = 1.62042(6)$ Å (1σ error limits). The observed bands were grouped into three band systems with $\Omega' = 7/2$ and four with $\Omega' = 3/2$, corresponding to the three $^2\Phi_{7/2}$ and four $^2\Pi_{3/2}$ states expected from the $1\sigma^2\ 2\sigma^2\ 1\pi^4\ 1\delta^3\ 3\sigma^1\ 2\pi^1$ and $1\sigma^2\ 2\sigma^2\ 1\pi^4\ 1\delta^2\ 3\sigma^2\ 2\pi^1$ electronic configurations. In addition, two interacting upper states with $\Omega' = 5/2$ were observed, one of which is thought to correspond to a $1\sigma^2\ 2\sigma^2\ 1\pi^3\ 1\delta^3\ 3\sigma^2\ 2\pi^1$, $^2\Delta_{5/2}$ state. Spectroscopic constants are reported for all of the observed states, and comparisons to related molecules are made. The ionization energy of OsN is estimated as IE(OsN) = 8.80 ± 0.06 eV. © *2011 American Institute of Physics*. [doi:10.1063/1.3633694]

I. INTRODUCTION

Transition metal molecules are of great interest and importance as catalysts in organic and organometallic chemistry.[1] Transition metal species are also of astrophysical[2,3] importance and have been identified in the atmospheres of M and S type stars and L type dwarfs,[4–7] where their spectra play a key role in the stellar classification scheme. Transition metal nitrides, in particular, are of importance in the fixation of nitrogen[8] and in the production of metallic thin films for optical applications[9,10] and for wear and corrosion resistance.[11–13] The interest in transition metal nitrides has prompted a number of spectroscopic investigations, with the result that spectra have now been obtained for all of the diatomic transition metal nitrides, MN, in the gas phase, with the exceptions of the 3*d* species MnN, CoN, NiN, CuN, and ZnN; the 4*d* species TcN, PdN, AgN, and CdN; and the 5*d* species AuN and HgN.[14] Infrared spectra of a large number of diatomic transition metal nitrides are also known from matrix isolation studies, including RuN and OsN.[15] It is interesting that the number of spectroscopically known species increases as one moves from the 3*d* series to the 4*d* series and on to the 5*d* series. This fact reflects the increasing ability of the transition metals to form strong π-bonds as one moves down the periodic table, due to the increasing size and accessibility of the n*d*π orbitals as n increases from 3 to 5.

Although gas-phase spectra of OsN are known,[16] the available spectra have only located the spin-forbidden $a\ ^4\Pi_{5/2} - X\ ^2\Delta_{5/2}$, $b\ ^4\Phi_{7/2} - X\ ^2\Delta_{5/2}$, and $b\ ^4\Phi_{5/2} - X\ ^2\Delta_{5/2}$ systems in the 8000–12 200 cm^{-1} region. In order to develop a more comprehensive understanding of the electronic structure of the OsN molecule, we have undertaken spectroscopic studies in the visible portion of the spectrum. In this article we report four excited states of $^2\Pi_{3/2}$ symmetry and three states of $^2\Phi_{7/2}$ symmetry, all of which are thought to result from the promotion of a nonbonding 1δ or 3σ electron into the antibonding 2π orbital.

In addition to OsN, two other osmium containing diatomic molecules are known: OsO, which is known from optical emission studies,[17] and OsC, which has been studied in this group by resonant two-photon ionization methods.[18] Recent work on the other 5*d* series transition metal nitrides includes HfN,[19] TaN,[20] WN,[21] ReN,[22,23] IrN,[24–26] and PtN.[27,28] These molecules are all of high interest as proving grounds for theoretical methods, due to the importance of properly treating relativistic and electron correlation effects. The large magnitude of the spin-orbit interaction in these species also makes accurate calculation of their properties a significant challenge for the *ab initio* quantum chemist.

II. EXPERIMENTAL

In the present work, resonant two-photon ionization (R2PI) spectroscopy with time of flight mass spectrometric detection was used to examine the optical spectroscopy of jet-cooled diatomic OsN using a previously described instrument.[29] Briefly, the molecule was produced by focusing a pulsed Nd: YAG laser (355 nm, 15 mJ/pulse) onto a vanadium-osmium alloy disk (45:55 mole percent V:Os), which was rotated and translated to prevent deep holes from being drilled into the sample. The laser-ablated metal atoms were entrained in a flow of helium carrier gas (120 psi) seeded with 5% ammonia. After traveling down a 1 cm long reaction zone, the gases expanded through a 2 mm orifice into a low pressure (2×10^{-4} Torr) vacuum chamber. The resulting supersonic expansion was roughly collimated by a 1 cm diameter skimmer and entered the ion source of a reflectron time of

a)Author to whom correspondence should be addressed. Electronic mail: morse@chem.utah.edu.

flight mass spectrometer.[30,31] In the ion source the molecular beam was exposed to tunable dye laser radiation that counter-propagated along the molecular beam path. After a delay of 20 ns, the output of an ArF (193 nm) excimer laser intersected the molecular beam at right angles. The ions produced by this process were accelerated in a Wiley-McLaren ion source and reflected onto a microchannel plate detector. The resulting ion signal was preamplified, digitized at 100 MHz, and stored using a personal computer for further processing. The entire experimental cycle was repeated at the rate of 10 Hz.

Survey spectra (at 0.15 cm^{-1} resolution) of the four most abundant isotopomers, $^{192}Os^{14}N$ (40.78% natural abundance), $^{190}Os^{14}N$ (26.26%), $^{189}Os^{14}N$ (16.12%), and $^{188}Os^{14}N$ (13.24%), were recorded from 19 200 to 23 900 cm^{-1}, and in isolated segments as far to the red as 12 900 cm^{-1}. Rotationally resolved spectra (at 0.04 cm^{-1} resolution) were obtained for the strongest vibrational transitions by inserting an air spaced etalon into the grating cavity of the dye laser and pressure scanning using sulfur hexafluoride (SF_6). Calibration of the rotationally resolved spectrum was achieved by simultaneously measuring the absorption spectrum of I_2 or isotopically pure $^{130}Te_2$. The I_2 or Te_2 lines were identified by comparison to the corresponding atlas,[32,33] which permitted the absolute calibration of the OsN spectra. In the final step, the molecular spectra were corrected for the Doppler shift experienced by the molecules as they traveled toward the radiation source at the beam velocity of the helium (1.77×10^5 cm/s) (Ref. 34) and for the –0.0056 cm^{-1} error in the I_2 atlas.[35] The total correction amounted to only 0.11–0.14 cm^{-1} for all of the examined bands.

The excited state lifetime of the principal isotopic modification, $^{192}Os^{14}N$, was measured by setting the dye laser radiation to the resonant frequency and varying the time at which it is fired. The ion signal was then recorded as a function of the excitation-ionization delay and fitted to an exponential decay curve using the Levenberg-Marquardt nonlinear least-squares algorithm.[36] For each band that was measured, three independent lifetime curves were collected and fitted, the fitted lifetimes were averaged, and the standard deviation of the three values is reported as the 1σ error limit.

III. RESULTS

A. Vibronic spectrum of OsN

Low resolution (0.15 cm^{-1}) survey scans were recorded for diatomic OsN in the 19 200–23 900 cm^{-1} region and at isolated wavenumber regions farther to the red using LDS 751, LDS 698, rhodamine 590, coumarin 540A, 500, 480, 460, 450, 440, and stilbene 420 laser dyes. The spectrum consists of more than 20 bands, and becomes somewhat more congested to the blue, where overlapping bands are observed. Seventeen of the bands that were observed were investigated at higher resolution and were successfully calibrated and analyzed. Figure 1 displays the vibronic spectrum of $^{192}Os^{14}N$, the most abundant isotope (40.85%). Seven band systems have been identified in Fig. 1, labeled systems B-H. The letter A is reserved for the as yet unobserved $1\sigma^2\ 2\sigma^2\ 1\pi^4\ 1\delta^4\ 3\sigma^1$, $^2\Sigma^+$ term, which is predicted to lie ~7500 cm^{-1} above the ground level. All of these systems have been determined

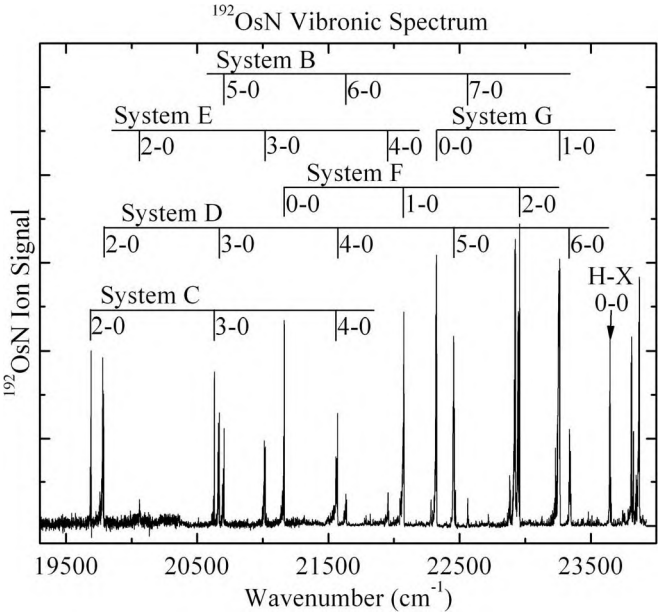

FIG. 1. Vibronic spectrum of OsN, with assigned band systems indicated.

to originate from the $^2\Delta_{5/2}$ ground state, which arises from the $1\sigma^2\ 2\sigma^2\ 1\pi^4\ 1\delta^3\ 3\sigma^2$ electronic configuration. All bands have a band head in the R branch, with the Q and P branches strongly red degraded, consistent with an increase in bond length upon electronic excitation.

The numbering of the vibrational bands was established by varying the assignment of v′, fitting the measured bands to obtain values of T_0, ω_e', and $\omega_e'x_e'$, and then computing the transition wavenumber as a function of a continuous parameter, v′, using the following equation:

$$\nu = T_0 + v'\omega_e' - (v'^2 + v')\omega_e'x_e'. \tag{3.1}$$

The corresponding isotope shift was calculated as a function of v′, as

$$\begin{aligned}\nu(^{188}Os\,^{14}N) - \nu(^{192}Os\,^{14}N) &= (\rho - 1)[\omega_e'(v' + 1/2) - \omega_e''(1/2)] - (\rho^2 - 1)\\ &\times [\omega_e'x_e'(v' + 1/2)^2 - \omega_e''x_e''(1/2)^2].\end{aligned} \tag{3.2}$$

Here, the $^{192}Os^{14}N$ isotope was used as the reference species, and the fitted values of T_0, ω_e', $\omega_e'x_e'$, were combined with the previously reported[16] values of ω_e'' and $\omega_e''x_e''$ to generate the isotope shift vs. transition wavenumber plot. The parameter, ρ, is given by $[\mu(^{192}Os^{14}N)/\mu(^{188}Os^{14}N)]^{1/2}$.[37] Plots of the resulting isotope shift vs. transition wavenumber generally provided a definitive vibrational numbering for the band systems, as illustrated in Fig. 2 for the C-X system. The sole exception is the weak B[16.0]3/2 ← X $^2\Delta_{5/2}$ system, for which only one band was rotationally resolved, and for which the vibrational numbering could be in error. No bands arising from any vibrational levels other than the v″ = 0 level of the X $^2\Delta_{5/2}$ ground state were observed.

Subsections III B–III H provide results for each of the observed band systems. In addition to the common designation of an upper state by a letter, we also adopt a designation in which the energy of the v′ = 0 level is expressed in thousands

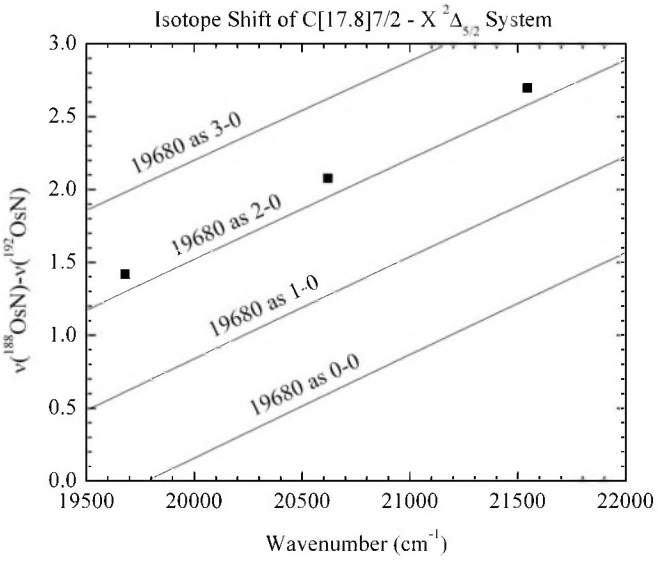

FIG. 2. Isotope shifts and vibrational numbering of the C-X system. From this analysis, it is evident that the 19 680 cm^{-1} band is the 2-0 band of the system.

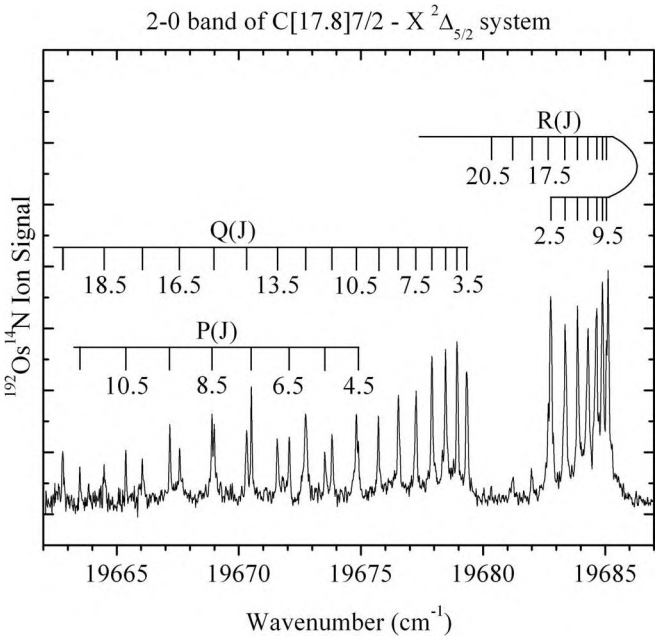

FIG. 3. Rotationally resolved spectrum of the 2-0 band of the C $^2\Phi_{7/2} \leftarrow X\,^2\Delta_{5/2}$ system.

of cm^{-1} in square brackets, along with the Ω' value. Thus, the C[17.8]7/2 state is the state with $\Omega' = 7/2$ whose T_0 value lies near 17 800 cm^{-1}. The letter designation is retained for easy reference. The rotational structure of all of the resolved bands could be fit to the expression

$$\nu = \nu_0 + B'J'(J'+1) - B''J''(J''+1) \tag{3.3}$$

to obtain values for ν_0, B′, and B″. Upper and lower state Ω values were determined by the first lines present in the spectrum.

Details not provided in this article are available through the Electronic Physics Auxiliary Publication Service (EPAPS) (Ref. 38) of the American Institute of Physics and also from the author (M.D.M.). This document provides rotationally resolved spectra for all bands that were investigated, along with line positions, rotational fits, and isotope shift plots that support the vibrational numbering provided for each band system.

Despite scans over the region where the 0-0 and 1-0 bands of the C [17.8]7/2 ← X $^2\Delta_{5/2}$ system were calculated to occur, these features were not observed in the spectrum. Indeed, no vibronic features were observed to the red of the C [17.8]7/2 ← X $^2\Delta_{5/2}$ 2-0 band at 19 680 cm^{-1}. We believe that these features are unobserved because the combination of the dye laser photon and the ArF excimer photon falls below the ionization limit of the molecule. The absence of the C-X 1-0 band, predicted to occur at 18 728 cm^{-1} and the presence of the C-X 2-0 band at 19 680 cm^{-1} then places the ionization energy of OsN in the range of 8.80 ± 0.06 eV. This is consistent with the high ionization energy of atomic osmium, IE(Os) = 8.438 eV.[39]

B. The C[17.8]$^2\Phi_{7/2} \leftarrow X^2\Delta_{5/2}$ system

The 2-0, 3-0, and 4-0 vibrational bands were observed, rotationally resolved, and analyzed for this band system. Measured band origins, rotational constants, and fitted vibrational (T_0, ω_e', $\omega_e'x_e'$) and rotational (B_e', α_e', r_e') parameters for the various isotopomers of OsN are listed in Table I. The rotationally resolved spectrum of the 2-0 band of $^{192}Os^{14}N$ is displayed in Fig. 3. All of the bands of this system are characterized by an intense R branch and weaker Q and P branches. The first lines of R(2.5), Q(3.5), and P(4.5) establish the Ω-values as $\Omega'' = 5/2$, $\Omega' = 7/2$.

With only three rotationally resolved bands, the three vibrational parameters, T_0, ω_e', and $\omega_e'x_e'$, are uniquely defined and no error estimate is possible. Ordinarily, one would expect significant errors in the extrapolation from the $v' = 2$ level to determine T_0, but in this case the excellent agreement between the various isotopomers for the values of T_0, ω_e', and $\omega_e'x_e'$ gives us confidence that these values are accurate. Likewise, the values of r_e', obtained from the fit of B_2', B_3', and B_4' to extract B_e' and α_e' are in very good agreement from isotope to isotope. A weighted average of the calculated values of r_e' for the various isotopomers provides $r_e' = 1.68146(15)$ Å, which is our best estimate of the actual bond length of the C state. This value is uncorrected for any **S**- or **L**-uncoupling interactions with other states,[40] but these are not expected to be significant due to the large spin-orbit splitting expected for this molecule.

The measured excited state lifetime for the $v' = 2$ and $v' = 3$ levels, 0.738 ± 0.031 μs and 0.808 ± 0.012 μs, respectively, is typical for excited states of transition metal molecules. If the only decay process is fluorescence to the ground electronic state, the relationship[41]

$$f = \frac{g_2}{g_1}\frac{1.51}{\nu_0^2\tau} \tag{3.4}$$

provides an estimate of the absorption oscillator strength of the C-X system as $f \approx 0.004$–0.005. These values suggest that the transition is an electronically allowed metal-centered excitation. If so, the assignment of the ground electronic state as

TABLE I. Spectroscopic constants for the C[17.8]$^2\Phi_{7/2}$ – X $^2\Delta_{5/2}$ system of OsN.

Band	Constant	$^{192}Os^{14}N$	$^{190}Os^{14}N$	$^{189}Os^{14}N$	$^{188}Os^{14}N$	τ (μs)
2-0	ν_0 (cm^{-1})	19 680.0008(22)	19 680.6951(27)	19 681.0735(22)	19 681.4181(29)	0.738(31)
	B'_2 (cm^{-1})	0.448884(27)	0.449076(33)	0.449355(29)	0.449523(35)	
	r'_2(Å)	1.696324(51)	1.696569(62)	1.696350(55)	1.696345(66)	
3-0	ν_0 (cm^{-1})	20 618.6759(21)	20 619.6994(28)	20 620.2285(68)	20 620.7522(29)	0.808(12)
	B'_3 (cm^{-1})	0.445763(34)	0.445907(30)	0.446417(50)	0.446307(27)	
	r'_3(Å)	1.702252(65)	1.702587(57)	1.701923(95)	1.702446(51)	
4-0	ν_0 (cm^{-1})	21 544.3000(79)	21 545.6608(105)	21 546.3529(73)	21 546.9949(143)	
	B'_4 (cm^{-1})	0.442566(94)	0.441960(80)	0.442392(53)	0.442900(115)	
	r'_4 (Å)	1.708389(181)	1.710173(155)	1.709648(102)	1.708982(222)	
	T_0 (cm^{-1})	17763.50	17763.56	17763.67	17763.48	
	ω'_e (cm^{-1})	977.83	978.13	978.25	978.61	
	$\omega'_e x'_e$ (cm^{-1})	6.53	6.52	6.52	6.55	
	B'_e (cm^{-1})	0.45679(9)	0.45810(91)	0.45824(127)	0.45783(22)	
	α'_e (cm^{-1})	0.00316(5)	0.00356(48)	0.00348(67)	0.00331(12)	
	r'_e (Å)	1.68157(16)	1.6798(17)	1.6798(23)	1.6809(4)	
X $^2\Delta_{5/2}$	B''_0 (cm^{-1})	0.491921(34)	0.492121(36)	0.492469(42)	0.492660(36)	
	r''_0 (Å)	1.620422(56)	1.620673(59)	1.620395(69)	1.620379(59)	

$^2\Delta_{5/2}$ requires that the C[17.8]7/2 state be dominated by $^2\Phi_{7/2}$ character.

C. The D[18.0]$^2\Pi_{3/2}$ ← X$^2\Delta_{5/2}$ system

Close to the bands of the C-X system, one finds another strong absorption system, the D[18.0]3/2 ← X$^2\Delta_{5/2}$ system. For this system, the 2-0, 3-0, 4-0, and 5-0 bands were rotationally resolved, calibrated, and analyzed. Although similar in intensity to the bands of the C-X system, the rotationally resolved bands of this system are somewhat different in appearance, as illustrated in Fig. 4. All of the bands of this system are characterized by a weak R branch, a stronger Q branch, and a P branch that is quite intense. This is visible even in the low-resolution spectra, where a distinct tailing to the red is visible due to the high intensity in the P lines. The first lines R(2.5), Q(2.5), and P(2.5) identify the Ω values as $\Omega'' = 5/2$, $\Omega' = 3/2$.

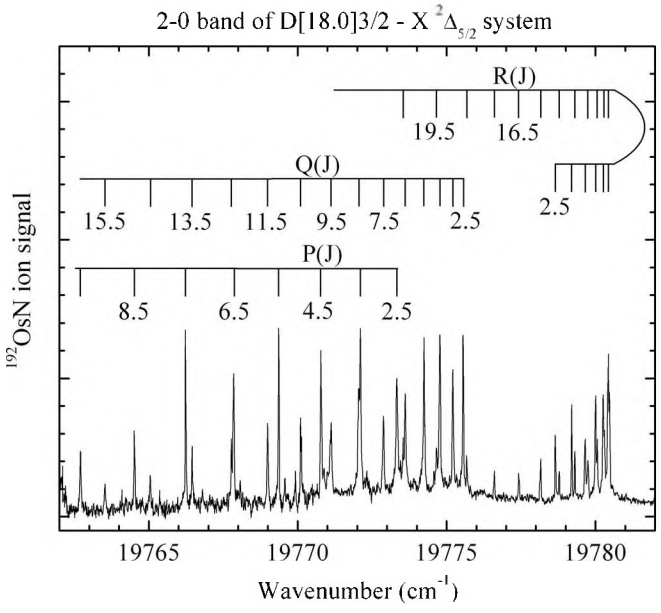

FIG. 4. Rotationally resolved spectrum of the 2-0 band of the D $^2\Pi_{3/2}$ ← X $^2\Delta_{5/2}$ system.

As was the case with the C system, the first band observed is the 2-0 band. Although one would ordinarily think that the observation and accurate fitting of 4 bands in this system (the 2-0, 3-0, 4-0, and 5-0) would allow an accurate determination of T_0, ω_e', and $\omega_e'x_e'$, in this case there is significant uncertainty in these parameters and significant variation in these values from isotope to isotope (see Table II). The difficulties in this system stem from the fact that the 3-0 band is perturbed, with the perturber state evident in the spectra of the ^{189}OsN and ^{188}OsN isotopes. Accordingly, this level is excluded from the fit of the band origins to obtain T_0, ω_e', and $\omega_e'x_e'$, and from the fit of the B_v' values to obtain B_e', α_e', and r_e' for these isotopes. Even though perturbations in the $v' = 3$ level are not apparent in the other isotopes, the fits to obtain T_0, ω_e', $\omega_e'x_e'$, B_e', α_e', and r_e' remain suspect for this state. Combining the results for all isotopes, however, a best estimate of r_e' for this state is 1.687 ± 0.003 Å.

Excited state lifetimes were measured for ^{192}OsN to be 1.17(11), 1.26(4), and 0.863(17) μs for the $v' = 2$, 3, and 5 levels of the D[18.0]3/2 state. Of these, the value for the unperturbed $v' = 2$ level is most likely to be representative of the electronic nature of this state. Assuming that fluorescence occurs solely to the ground X$^2\Delta_{5/2}$, $v'' = 0$ level, the 1.17 μs lifetime converts to an absorption oscillator strength of $f \approx 0.003$, suggesting an electronically allowed metal-based excitation. This suggests that the D[18.0]3/2 state is primarily of $^2\Pi_{3/2}$ character.

D. The F[21.2]$^2\Phi_{7/2}$ ← X$^2\Delta_{5/2}$ system

Moving further to the blue, a 0-0 band is found near 21 151 cm^{-1}. The corresponding 1-0 and 2-0 bands are found near 22 062 and 22 944 cm^{-1}, respectively. This system is identified as the F[21.2]7/2 ← X$^2\Delta_{5/2}$ system on the basis of

TABLE II. Spectroscopic constants for the D[18.0]$^2\Pi_{3/2}$ – X $^2\Delta_{5/2}$ system of OsN.

Band	Constant	$^{192}Os^{14}N$	$^{190}Os^{14}N$	$^{189}Os^{14}N$	$^{188}Os^{14}N$	τ (μs)
2-0	ν_0 (cm^{-1})	19 775.9842(22)	19 776.5575(20)	19 776.8575(23)	19 777.1537(18)	1.17(11)
	B'_2 (cm^{-1})	0.443198(28)	0.443391(34)	0.443691(29)	0.443864(36)	
	r'_2(Å)	1.707171(54)	1.707411(65)	1.707144(56)	1.707125(69)	
3-0	ν_0 (cm^{-1})	20 657.6998(22)	20 658.9758(26)	20 658.9902(56)	20 659.6125(63)	1.26(4)
	B'_3 (cm^{-1})	0.437158(69)	0.437205(62)	0.437150(122)	0.438055(104)	
	r'_3 (Å)	1.718924(136)	1.719447(122)	1.719868(240)	1.718407(204)	
3-0[a]	ν_0 (cm^{-1})			20 659.6166(37)	20 660.2533(36)	
	B'_3 (cm^{-1})			0.437498(117)	0.437678(65)	
	r'_3 (Å)			1.719184(230)	1.719146(128)	
4-0	ν_0 (cm^{-1})	21 558.0923(33)	21 559.2877(38)	21 559.8942(37)	21 560.5073(29)	
	B'_4 (cm^{-1})	0.432417(32)	0.432614(42)	0.432811(37)	0.433072(40)	
	r'_4 (Å)	1.728321(64)	1.728547(84)	1.728467(74)	1.728264(80)	
5-0	ν_0 (cm^{-1})	22 446.6492(22)	22 449.0627(40)	22 450.6445(59)	22 447.3434(35)	0.863(17)
	B'_5 (cm^{-1})	0.429767(40)	0.430360(105)	0.431275(203)	0.430365(101)	
	r'_5 (Å)	1.733642(81)	1.733068(211)	1.731543(408)	1.733691(203)	
	T_0 (cm^{-1})	18 009.08(39.16)	18 009.96(36.49)	17 991.77	17 980.89	
	ω'_e (cm^{-1})	877.56(27.46)	877.07(25.59)	893.31	902.97	
	$w'_e x'_e$ (cm^{-1})	−1.71(3.41)	−1.84(3.18)	0.256	1.61	
	B'_e (cm^{-1})	0.45365(248)	0.45337(288)	0.45394(464)	0.45505(320)	
	α'_e (cm^{-1})	0.00450(120)	0.00437(140)	0.00432(220)	0.00463(151)	
	r'_e (Å)	1.6874(46)	1.6885(54)	1.6878(86)	1.6860(59)	
X $^2\Delta_{5/2}$	B''_0 (cm^{-1})	0.491921(34)	0.492121(36)	0.492469(42)	0.492660(36)	
	r''_0 (Å)	1.620422(56)	1.620673(59)	1.620395(69)	1.620379(59)	

[a]A second feature was observed in the spectra of the $^{189}Os^{14}N$ and $^{188}Os^{14}N$ isotopes; this was fitted and is included in this table.

rotationally resolved spectra of all three bands. The rotationally resolved spectra are quite similar to the 2-0 band of the C-X system that is displayed in Fig. 3. As in the C-X system, this system exhibits a strong R branch beginning with R(2.5), a somewhat weaker Q branch beginning with Q(3.5), and a much weaker P branch beginning with P(4.5). These values establish the system as a $\Omega' = 7/2 \leftarrow \Omega'' = 5/2$ system.

The fitted spectroscopic constants listed in Table III show excellent agreement between isotopes, and display the expected trends as the reduced mass varies. The only odd aspect of this system is the extremely high anharmonicity, which probably signals some sort of global perturbation. This is reflected in a failure of the Pekeris relationship,[42] which is valid for a Morse potential, and provides

$$\alpha_e = \frac{6(\omega_e x_e B_e^3)^{1/2}}{\omega_e} - \frac{6B_e^2}{\omega_e}. \quad (3.5)$$

Although this relationship predicts values of α_e that are in good agreement with the measured values for the C[17.8]7/2 state, it is in error by 26% for the F[21.2]7/2 state, indicating that the system is either perturbed by interaction with another state or that its potential energy curve departs significantly from the form of the Morse potential. Nevertheless, extrapolation of the measured B_v' values provides values of B_e' that are in good agreement between isotopes and provide an isotopically averaged value of r_e' of 1.6920(2) Å for this state.

Decay lifetimes have been measured for the $v' = 0$ and $v' = 1$ levels, giving values of 1.13(4) and 1.41(3) μs, respectively. Assuming fluorescence solely to the ground $X^2\Delta_{5/2}$ state, these provide estimates of the absorption oscillator strength of this system of $f \approx 0.0025$. This suggests that the system is electronically allowed, and that the F[21.2]7/2 state is dominated by $^2\Phi_{7/2}$ character.

E. The G[22.3]$^2\Phi_{7/2} \leftarrow X^2\Delta_{5/2}$ system

Considerably further to the blue lies the intense G[22.3]7/2 $\leftarrow X^2\Delta_{5/2}$ band system. The 0-0 and 1-0 bands, which lie near 22 309 and 23 248 cm^{-1}, respectively, have been rotationally resolved, calibrated, and analyzed. The overall appearance of these bands is very similar to that of the 2-0 band of the C-X system, displayed in Fig. 3. Like the C-X and F-X systems, this system displays an intense R branch beginning with R(2.5), a weaker Q branch beginning with Q(3.5), and a much weaker P branch beginning with P(4.5). These first lines establish the values $\Omega'' = 5/2$, $\Omega' = 7/2$. Fitted spectroscopic constants are provided in Table IV.

With only two bands observed, it is impossible to extract values of ω_e' and $\omega_e'x_e'$; only $\Delta G'_{1/2}$ can be reported. However, it is possible to obtain B_e', α_e', and r_e' from the data. The signal for the 1-0 band was too weak to observe the minor isotopes ^{189}OsN and ^{188}OsN, however. A weighted average of the r_e' values for the ^{192}OsN and ^{190}OsN isotopes, provides our best estimate of r_e' for this state, $r_e' = 1.6967$ Å. The vibrational interval, $\Delta G'_{1/2}$, is 938.16 cm^{-1} for the ^{192}OsN isotopic modification.

The lifetime of the $v' = 0$ level is measured to be 0.760(24) μs. Assuming a decay pathway consisting solely of fluorescence to the ground state, this converts to an absorption oscillator strength of $f \approx 0.004$. Based on the intensity of the band system, it seems likely that this is again an

TABLE III. Spectroscopic constants for the F[21.2] $^2\Phi_{7/2}$ – X $^2\Delta_{5/2}$ system of OsN.

Band	Constant	$^{192}Os^{14}N$	$^{190}Os^{14}N$	$^{189}Os^{14}N$	$^{188}Os^{14}N$	τ (μs)
0-0	ν_0 (cm^{-1})	21 151.0458(25)	21 151.0278(23)	21 151.0312(25)	21 151.0169(22)	1.13(4)
	B'_0 (cm^{-1})	0.448756(20)	0.448933(23)	0.449214(33)	0.449442(30)	
	r'_0 (Å)	1.696566(38)	1.696839(43)	1.696617(62)	1.696498(57)	
1-0	ν_0 (cm^{-1})	22 061.5216(32)	22 061.8169(27)	22 061.9801(37)	22 062.1253(31)	1.41(3)
	B'_1 (cm^{-1})	0.444218(30)	0.444431(36)	0.444724(34)	0.444942(40)	
	r'_1 (Å)	1.705210(58)	1.705412(69)	1.705160(65)	1.705056(77)	
2-0	ν_0 (cm^{-1})	22 943.9328(30)	22 944.5385(30)	22 944.8485(33)	22 945.1526(27)	
	B'_2 (cm^{-1})	0.439334(32)	0.439474(51)	0.439792(41)	0.439972(26)	
	r'_2(Å)	1.714662(62)	1.715003(100)	1.714694(80)	1.714659(51)	
	T_0 (cm^{-1})	21 151.04	21 151.03	21 151.03	21 151.02	
	ω'_e (cm^{-1})	938.54	938.86	939.03	939.19	
	$\omega'_e x'_e$ (cm^{-1})	14.03	14.03	14.04	14.04	
	B'_e (cm^{-1})	0.45117(21)	0.45137(28)	0.45164(27)	0.45189(29)	
	α'_e (cm^{-1})	0.00471(16)	0.00473(21)	0.00471(20)	0.00474(21)	
	r'_e(Å)	1.6920(4)	1.6922(5)	1.6920(5)	1.6919(5)	
X $^2\Delta_{5/2}$	B''_0 (cm^{-1})	0.491921(34)	0.492121(36)	0.492469(42)	0.492660(36)	
	r''_0 (Å)	1.620422(56)	1.620673(59)	1.620395(69)	1.620379(59)	

electronically allowed absorption system, in which the G[22.3]7/2 state is dominated by $^2\Phi_{7/2}$ electronic character.

F. The E[18.1]$^2\Pi_{3/2}$ ← X$^2\Delta_{5/2}$ system

A weaker band system than those previously described is the E[18.1]3/2 ← X $^2\Delta_{5/2}$ system. For this system, only the 3-0 band was rotationally resolved and analyzed. The band is similar in structure to the D-X 2-0 band shown in Fig. 4. The R branch is relatively weak, the Q branch more intense, and the P branch more intense still, consistent with a $\Delta\Omega = -1$ transition. The first lines of R(2.5), Q(2.5), and P(2.5) confirm this fact, demonstrating that this is a $\Omega' = 3/2 \leftarrow \Omega'' = 5/2$ transition.

With only a single band of the system rotationally resolved, accurate determinations of T_0, ω_e', $\omega_e' x_e'$, B_e', α_e', and r_e' are impossible. The values of r_3' determined for the four most abundant isotopes from this band are in good agreement, however, providing a weighted average value of 1.7068 Å. Low resolution measurements of the band heads of the 2-0 and 4-0 bands, along with the results of the rotationally resolved study of the 3-0 band, are reported in Table V. Using the measured band heads to estimate the locations of the corresponding band origins, we have been able to estimate the values of T_0, ω_e', and $\omega_e' x_e'$ for the ^{192}OsN and ^{190}OsN isotopomers. The results for the two isotopes are in good agreement considering the indirect procedure that was employed. Finally, if we assume that the Pekeris relationship, Eq. (3.5), is obeyed, the estimated values of ω_e' and $\omega_e' x_e'$ may be combined with the measured value of B_3' to provide estimates of B_e', α_e', and r_e' for the ^{192}OsN and ^{190}OsN isotopomers. The resulting values for ^{192}OsN and ^{190}OsN, 1.6828 and 1.6840 Å, are in good agreement for such an indirect method, and provide our best estimate of the equilibrium bond length of the E[18.1]3/2 state.

The lifetimes of the $v' = 2$ and $v' = 3$ levels of the E state were measured to be 0.551(58) and 0.703(52) μs, respectively, values that are comparable to that found for the much more intense G state. The fact that the E state shows up rather weakly in the spectrum but undergoes rapid

TABLE IV. Spectroscopic constants for the G[22.3] $^2\Phi_{7/2}$ – X $^2\Delta_{5/2}$ system of OsN.

Band	Constant	$^{192}Os^{14}N$	$^{190}Os^{14}N$	$^{189}Os^{14}N$	$^{188}Os^{14}N$	τ (μs)
0-0	ν_0 (cm^{-1})	22 309.4871(25)	22 309.5070(24)	22 309.5127(51)	22 309.5316(28)	0.760(24)
	B'_0 (cm^{-1})	0.447050(43)	0.447192(48)	0.447557(59)	0.447724(48)	
	r'_0(Å)	1.699800(82)	1.700139(91)	1.699754(112)	1.699750(91)	
1-0	ν_0 (cm^{-1})	23 247.6424(24)	23 247.9937(32)			
	B'_1 (cm^{-1})	0.443843(12)	0.444044(18)			
	r'_1(Å)	1.705930(23)	1.706155(35)			
	T_0 (cm^{-1})	22 309.49	22 309.51			
	$\Delta G'_{1/2}$ (cm^{-1})	938.16	938.14			
	B'_e (cm^{-1})	0.44865	0.44905			
	α'_e (cm^{-1})	0.00321	0.00372			
	r'_e (Å)	1.6968	1.6966			
X $^2\Delta_{5/2}$	B''_0 (cm^{-1})	0.491921(34)	0.492121(36)	0.492469(42)	0.492660(36)	
	r''_0(Å)	1.620422(56)	1.620673(59)	1.620395(69)	1.620379(59)	

TABLE V. Spectroscopic constants for the E[18.1] $^2\Pi_{3/2}$ – X $^2\Delta_{5/2}$ system of OsN.[a]

Band	Constant	$^{192}Os^{14}N$	$^{190}Os^{14}N$	$^{189}Os^{14}N$	$^{188}Os^{14}N$	τ (μs)
2-0	Band Head	20 061.0	20 060.9			0.551(58)
3-0	ν_0 (cm^{-1})	21 006.1985(18)	21 007.1362(29)	21 007.6218(33)	21 008.0887	0.703(52)
	B'_3 (cm^{-1})	0.443446(19)	0.443602(26)	0.443944(36)	0.444168(41)	
	r'_3(Å)	1.706693(37)	1.707005(50)	1.706657(69)	1.706541(79)	
3-0[b]	ν_0 (cm^{-1})			21 007.1361(27)	21 007.6339(34)	
	B'_3 (cm^{-1})			0.443905(37)	0.444045(41)	
	r'_3(Å)			1.706732(71)	1.706777(79)	
4-0	Band Head	21 950.3	21 950.2	21 950.9	21 951.3	
	T_0 (cm^{-1})	18 103.5	18 107.8			
	ω_e' (cm^{-1})	995.1	992.3			
	$\omega_e x_e'$ (cm^{-1})	6.9	6.5			
	α_e' (cm^{-1})	0.003625	0.003488			
	B_e' (cm^{-1})	0.45613	0.45581			
	r_e' (Å)	1.6828	1.6840			
X $^2\Delta_{5/2}$	B''_0 (cm^{-1})	0.491921(34)	0.492121(36)	0.492469(42)	0.492660(36)	
	r''_0(Å)	1.620422(56)	1.620673(59)	1.620395(69)	1.620379(59)	

[a]The vibrational fit to determine T_0, ω_e', and $\omega_e'x_e'$ is based on estimated band origin positions of the 2-0 and 4-0 bands, along with the fitted value of the band origin of the 3-0 band. The Pekeris relationship, Eq. (3.5) was then assumed to be valid and used in conjunction with the values of ω_e', $\omega_e'x_e'$, and B_3' to estimate α_e', B_e', and r_e'. The 2-0 band was not identifiable in the spectra of the minor isotopes, $^{189}Os^{14}N$ and $^{188}Os^{14}N$.
[b]A second feature was observed in spectra of the $^{189}Os^{14}N$ and $^{188}Os^{14}N$ isotopes; this was fitted and is included in this table.

fluorescence suggests that the primary decay pathway is fluorescence to a state other than the ground state. Low-lying electronic states to which the E state might fluoresce include the $1\sigma^2\ 2\sigma^2\ 1\pi^4\ 1\delta^4\ 3\sigma^1$, A $^2\Sigma^+$ state, calculated to lie near 4500 cm^{-1} (7500 cm^{-1} including the spin-orbit stabilization of the $X^2\Delta_{5/2}$ ground state), but not yet experimentally known, and the $1\sigma^2\ 2\sigma^2\ 1\pi^4\ 1\delta^3\ 3\sigma^1\ 2\pi^1$, $a\,^4\Pi$ and $b\,^4\Phi$ states, lying near 8400 and 11 000 cm^{-1}, respectively.[16] On this basis, a dispersed fluorescence study of the emission from the E[18.1]3/2 state might be useful for locating these low-lying excited states.

G. The B[16.0]$^2\Pi_{3/2}$ ← X$^2\Delta_{5/2}$ system

Similar in intensity to the E[18.1]3/2 ← X $^2\Delta_{5/2}$ system is the weak B[16.0]3/2 ← X $^2\Delta_{5/2}$ system. The only member of this system to be rotationally resolved is the 20 694 cm^{-1} band, which is similar in structure to the D-X 2-0 band that is displayed in Fig. 4. The upper level of this transition lies only 36 cm^{-1} above the D[18.0]3/2 v′ = 3 level; it is possible that some mixing of these two levels allows this band to borrow intensity from the D-X system. Alternatively, it may be that the greater intensity of this band is simply due to better Franck-Condon factors than the higher-lying bands of the B-X system. The first lines of R(2.5), Q(2.5), and P(2.5) identify the band as a $\Omega' = 3/2 \leftarrow \Omega'' = 5/2$ transition, a fact that is confirmed by the relative intensities of the branches.

In addition to the 20 694 cm^{-1} band, the low resolution scans also show features of this system near 21 630 and 22 558 cm^{-1}, respectively. The vibrational assignment of this system is uncertain due to limited and inconsistent isotope shift data. Although the data is best explained by assigning the 20 694 cm^{-1} band as the 5-0 band, it is possible that this numbering is in error, particularly if the band positions are shifted in an isotopically dependent manner by interactions with the D[18.0]$^2\Pi_{3/2}$ state. It is also troubling that the 4-0 band, which is predicted by the fit to lie between the C-X 2-0 and D-X 2-0 bands, is either extremely weak or completely absent. Nevertheless, assuming that the 20 694 cm^{-1} band is the 5-0 band, using the band heads of the 6-0 and 7-0 bands, and making a correction for the likely band origin positions, we are able to estimate the values of T_0, ω_e', and $\omega_e'x_e'$ for the more abundant ^{192}OsN and ^{190}OsN species, as provided in Table VI. These values, in combination with the measured values of B_5', were also used to estimate α_e', B_e', and r_e' using the Pekeris relationship (Eq. (3.5)). Although imperfect, this method allows an estimate of r_e', which when averaged over the ^{192}OsN and ^{190}OsN isotopes gives $r_e' \approx 1.706$ Å.

The measured lifetime of the v′ = 5 level, 1.26(12) μs, is completely in line with that found for the other band systems. Unlike the E-X system, however, the weak intensity of this band system might be explained by the fact that only the v′ = 5–7 levels are observed. These levels have poor Franck-Condon factors due to the large change in vibrational number upon excitation. It is likely that the 0-0, 1-0, 2-0, and 3-0 bands are more intense, but fall too low in energy to be observed unless a more energetic ionization photon is employed.

These considerations do not explain why the 4-0 band is unobserved, however. The 4-0 band is predicted, based on the fit, to fall slightly to the red of the D-X 2-0 band, near 19 758 cm^{-1}. One would expect it to be more intense than the 5–0 band, on the basis of Franck-Condon factors. If the B-X system is allowed, but also borrows intensity from the D-X system, however, then it is possible that the borrowed transition moment is of opposite sign to the intrinsic transition moment, and that a cancellation of the two moments causes the 4-0 band to vanish. Although such an explanation is purely hypothetical at this point, the high relative intensity of the 5-0

TABLE VI. Spectroscopic constants for the B[16.0] $^2\Pi_{3/2}$ – X $^2\Delta_{5/2}$ system of OsN.[a]

Band	Constant	$^{192}Os^{14}N$	$^{190}Os^{14}N$	$^{189}Os^{14}N$	$^{188}Os^{14}N$	τ (μs)
5-0	ν_0 (cm^{-1})	20 694.0886(21)	20 695.5895(26)	20 696.3616(25)	20 697.1415(27)	1.26(12)
	B'_5 (cm^{-1})	0.436830(18)	0.437024(24)	0.437363(50)	0.437585(28)	
	r'_5(Å)	1.719569(35)	1.719803(47)	1.719449(98)	1.719329(55)	
6-0	Band Head	21 629.8	21 632.0	21 633.2	21 634.6	
7-0	Band Head	22 558.1	22 560.9			
	T_0 (cm^{-1})	15 978.7	15 974.5			
	ω_e' (cm^{-1})	954.0	955.6			
	$\omega_e'x_e'$ (cm^{-1})	1.8	1.9			
	α_e' (cm^{-1})	0.001256	0.001324			
	B_e' (cm^{-1})	0.44374	0.44430			
	r_e' (Å)	1.7061	1.7057			
X $^2\Delta_{5/2}$	B''_0 (cm^{-1})	0.491921(34)	0.492121(36)	0.492469(42)	0.492660(36)	
	r''_0(Å)	1.620422(56)	1.620673(59)	1.620395(69)	1.620379(59)	

[a] The vibrational fit to determine T_0, ω_e', and $\omega_e'x_e'$ is based on estimated band origin positions of the 6-0 and 7-0 bands, along with the fitted value of the band origin of the 5-0 band. The Pekeris relationship, Eq. (3.5) was then assumed to be valid and used in conjunction with the values of ω_e', $\omega_e'x_e'$, and B_5' to estimate α_e', B_e', and r_e'. Although this procedure is imprecise, and is compromised by errors in the determination of the vibrational parameters, particularly $\omega_e'x_e'$, it nevertheless provides an estimate of r_e'. The 7-0 band was not identifiable in the spectra of the minor isotopes, $^{189}Os^{14}N$ and $^{188}Os^{14}N$.

band is consistent with this explanation. The vibrational levels assigned as $v' = 4$ and $v' = 5$ lie below and above the $v' = 2$ and $v' = 3$ levels of the D[18.0]$^2\Pi_{3/2}$ state, respectively. Given that the first order perturbation theory correction to the wavefunction mixes in D[18.0]$^2\Pi_{3/2}$ character according to the expression

$$\Psi^{(1)}_{Bv_B} = \frac{H'_{Dv_D,Bv_B}}{E^{(0)}_{Bv_B} - E^{(0)}_{Dv_D}} \Psi^{(0)}_{Dv_D}, \tag{3.6}$$

the denominator will change sign in going from the B, $v' = 4 \sim$ D, $v' = 2$ perturbation to the B, $v' = 5 \sim$ D, $v' = 3$ perturbation. If the numerator retains the same sign, then the contribution for the first order correction to the wavefunction is positive for one case and negative for the other. Thus, the intrinsic and borrowed transition moments will tend to cancel for one level (the 4-0 band) and add constructively for the other (the 5-0 band). This could explain our inability to observe the B-X 4-0 band while simultaneously observing an anomalously high intensity for the B-X 5-0 band.

For the present, we identify the B state as the B[16.0]$^2\Pi_{3/2}$ state, with the recognition that although the Ω value of this state is definite, the Λ-S term symbol of the leading contribution to this state could be different from $^2\Pi$.

H. Additional bands

Three additional bands were rotationally resolved and are listed in Table VII. These consist of two $\Omega' = 5/2 \leftarrow \Omega'' = 5/2$ bands located near 22 911.5 and 22 934.0 cm^{-1} and an intense $\Omega' = 3/2 \leftarrow \Omega'' = 5/2$ band near 23 636.5 cm^{-1}. The latter band displays a small isotope shift, 0.0942 cm^{-1} for $\nu(^{188}OsN)$–$\nu(^{192}OsN)$, and is presumably the 0-0 band of a system that continues beyond the range investigated here. Accordingly, it is designated as the 0-0 band of the H[23.6]$^2\Pi_{3/2}$ $\leftarrow$ X $^2\Delta_{5/2}$ system. The H[23.6]$^2\Pi_{3/2}$ state is notable for having a significantly shorter bond length than any of the other excited states reported in this study. Only the ground state and the previously reported $1\sigma^2\ 2\sigma^2\ 1\pi^4\ 1\delta^3\ 3\sigma^1\ 2\pi^1$, $^4\Pi_{5/2}$, and $^4\Phi_{5/2,\ 7/2}$ states have bond lengths that are shorter than that of the H[23.6]$^2\Pi_{3/2}$ state.

The two bands near 22 911.5 and 22 934.5 cm^{-1} are the only bands examined in this study that have upper states with

TABLE VII. Spectroscopic constants for additional bands of OsN.

Band	Constant	$^{192}Os^{14}N$	$^{190}Os^{14}N$	$^{189}Os^{14}N$	$^{188}Os^{14}N$
H[23.6] $^2\Pi_{3/2} \leftarrow X^2\Delta_{5/2}$	ν_0 (cm^{-1})	23 636.5418(27)	23 636.5833(28)	23 636.6162(32)	23 636.6360(33)
0-0 band	B'_0 (cm^{-1})	0.465101(31)	0.465328(50)	0.465629(29)	0.465777(25)
	r'_0(Å)	1.666488(56)	1.666679(90)	1.666443(52)	1.666484(45)
$\Omega' = 5/2 \leftarrow X^2\Delta_{5/2}$	ν_0 (cm^{-1})	22 934.0221(36)	22 934.1918(44)		22 934.4026(41)
22 934 band	B' (cm^{-1})	0.440888(28)	0.441115(32)		0.441394(42)
	r' (Å)	1.711637(54)	1.711810(62)		1.711895(81)
$\Omega' = 5/2 \leftarrow X^2\Delta_{5/2}$	ν_0 (cm^{-1})	22 911.4990(43)	22 911.6572(37)	22 911.6825(92)	22 911.8299(42)
22 911 band	B' (cm^{-1})	0.440896(32)	0.441353(32)	0.442478(118)	0.442087(60)
	r' (Å)	1.711622(62)	1.711348(62)	1.709482(228)	1.710552(116)
X $^2\Delta_{5/2}$	B''_0 (cm^{-1})	0.491921(34)	0.492121(36)	0.492469(42)	0.492660(36)
	r''_0(Å)	1.620422(56)	1.620673(59)	1.620395(69)	1.620379(59)

$\Omega' = 5/2$. Moreover, they are separated by only 22.5 cm^{-1} and have remarkably similar values of B′: 0.44090 and 0.44089 cm^{-1}, respectively, for the ^{192}OsN isotopic form. The measured isotope shifts, $\nu(^{188}OsN)$–$\nu(^{192}OsN)$, are also quite similar, 0.3309 and 0.3805 cm^{-1}, for the two bands, respectively. The value of the measured isotope shift falls midway between that expected for a 0-0 band, which is typically –0.10 to –0.03 cm^{-1}, and that expected for a 1-0 band, which is typically 0.5–0.7 cm^{-1}.

The similarity of the upper states of these two bands suggests that they arise from a pair of $\Omega' = 5/2$ levels that are coupled by a homogeneous perturbation with a J-independent coupling matrix element, H_{12}, that is much larger than the separation between the interacting states. In such a case, examination of the two-state perturbation model shows that the effective band origins (ν_0) and effective rotational constants (B) of the two states are related to the term energies (T_0^+ and T_0^-) and rotational constants (B^+ and B^-) of the upper (+) and lower (−) of the states prior to interaction according to

$$\nu_0 = 1/2(T_0^+ + T_0^-) \pm H_{12} \pm (T_0^+ - T_0^-)^2/8H_{12} + \cdots \tag{3.7}$$

and

$$B = 1/2(B^+ + B^-) \pm (T_0^+ - T_0^-)(B^+ - B^-)/4H_{12} + \cdots. \tag{3.8}$$

In the limit that $|H_{12}| \gg |T_0^+ - T_0^-|$, these results predict that the two measured states will have the same effective value of B, which will be the average of the B values of the two states prior to interaction. In the same limit, the two band origins will be separated by $2H_{12}$, suggesting that in our case $H_{12} \approx 11$ cm^{-1}. Further, since the two measured band origins are displaced by $\pm H_{12}$ from the average of T^+ and T^-, they will display an isotope shift that is the average of the two states prior to interaction. This suggests that our two interacting states are $v' = 0$ and $v' = 1$ levels, leading to isotope shifts that are midway between that expected for levels with $v' = 0$ and $v' = 1$, as found. The fact that no $\Omega' = 5/2 \leftarrow X^2\Delta_{5/2}$ transition is observed where the 0-0 transition would be expected, roughly 800–1000 cm^{-1} to the red of these bands, suggests that $v' = 1$ level belongs to a dark state that gains its intensity via mixing with the $v' = 0$ level of a bright state. If this is true, dispersed fluorescence from these strongly mixed bands could terminate on both the doublet and the quartet manifolds, allowing the electronic structure of OsN to be probed more deeply.

IV. DISCUSSION

A. Assignment of observed states to configurations and terms

With the spectroscopic data described in Sec. III in hand, it is appropriate to try to identify the observed states with electronic configurations in the OsN molecule. Toward this end, a discussion of the molecular orbital structure of the molecule is useful. Figure 5 presents a qualitative molecular orbital diagram that is consistent with what was obtained via complete active space self-consistent field calculations in a previous study.[16] Ignoring the core-like 1σ orbital, which is primarily

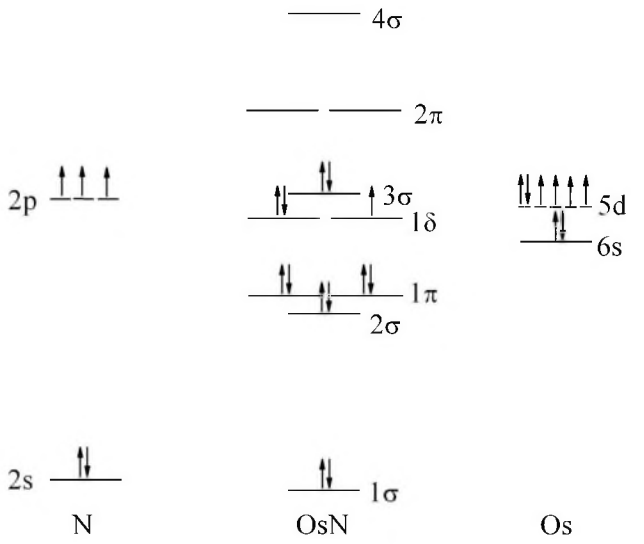

FIG. 5. Qualitative molecular orbital diagram for OsN.

nitrogen 2*s* in character, the remaining orbitals fall into three categories: (1) strongly bonding combinations of 2*p* orbitals on nitrogen and 5*d* orbitals on osmium, giving rise to the 2σ and 1π orbitals; (2) nonbonding orbitals consisting primarily of the 5*d*δ orbitals of osmium (forming the 1δ molecular orbital) and the 6*s* orbital of osmium (forming, with some admixture of the 5*d*σ and 6*p*σ osmium orbitals, the 3σ molecular orbital); and (3) strongly antibonding combinations of 2*p* orbitals on nitrogen and 5*d* orbitals on osmium, giving rise to the 2π and 4σ antibonding molecular orbitals.

The ground electronic configuration, $1\sigma^2\ 2\sigma^2\ 1\pi^4\ 1\delta^3\ 3\sigma^2$, places a single hole in the nonbonding 1δ set of orbitals, leading only to an inverted $^2\Delta$ term with a $^2\Delta_{5/2}$ ground level. If the hole is instead placed in the nonbonding 3σ orbital, a $1\sigma^2\ 2\sigma^2\ 1\pi^4\ 1\delta^4\ 3\sigma^1$, $^2\Sigma^+$ state is obtained. This is predicted to be the first excited state of the molecule, calculated to lie 4465 cm^{-1} above the average of the $X_1\ ^2\Delta_{5/2}$ and $X_2\ ^2\Delta_{3/2}$ levels.[16] The spin-orbit interaction, which is quite significant in heavy atoms such as Os, shifts the $X_1\ ^2\Delta_{5/2}$ level to lower energies by the amount –A, where A is approximately given by $\zeta_{5d}(Os) \approx 3045$ cm^{-1}; thus, the $^2\Sigma^+$ state may be expected to lie ~7500 cm^{-1} above the $X_1\ ^2\Delta_{5/2}$ ground level. This prediction, of course, ignores any inaccuracies in the calculation as well as off-diagonal spin-orbit interactions, which are important in second order perturbation theory.

The next higher energy configurations arise from the ground state by promotion of either a 3σ or 1δ nonbonding electron to the 2π antibonding orbital, giving the $1\sigma^2\ 2\sigma^2\ 1\pi^4\ 1\delta^3\ 3\sigma^1\ 2\pi^1$ and $1\sigma^2\ 2\sigma^2\ 1\pi^4\ 1\delta^2\ 3\sigma^2\ 2\pi^1$ configurations. The former configuration leads to the $a\ ^4\Pi$ and $b\ ^4\Phi$ states that have been identified by Fourier transform emission spectroscopy,[16] along with two $^2\Pi$ and two $^2\Phi$ terms. Both $^2\Pi$ and $^2\Phi$ states are accessible under electric dipole-allowed transitions from the $X\ ^2\Delta$ ground state. Similarly, the $1\sigma^2\ 2\sigma^2\ 1\pi^4\ 1\delta^2\ 3\sigma^2\ 2\pi^1$ configuration generates one $^4\Pi$ term, two $^2\Pi$ terms, one $^2\Phi$ term, and one ^{2}H term. Thus, the promotion of a nonbonding 1δ or 3σ electron to the antibonding 2π orbital will lead to four $^2\Pi$ terms and three $^2\Phi$ terms that may be accessed in fully allowed optical transitions. In transitions

TABLE VIII. Summary of all experimentally known states of $^{192}Os^{14}N$.

	Experiment				Theory[a]		
State	T_0 (cm^{-1})	r_e (Å)	ω_e (cm^{-1})	$\omega_e x_e$ (cm^{-1})	T_0 (cm^{-1})	r_e (Å)	ω_e (cm^{-1})
$X\ ^2\Delta_{5/2}$	0.00	1.6180[a]	1147.95[a]	5.460[a]	0.00	1.627	1146
$a\ ^4\Pi_{5/2}$	8381.75[a]	1.6552[a]	1045.61[a,b]		8445	1.677	1003
$b'\ ^4\Phi_{7/2}$	11 147.93[a]	1.6679[a,c]			10 245	1.675	1004
$b\ ^4\Phi_{5/2}$	12 127.19[a]	1.6591[a,c]			10 245	1.675	1004
$B\ ^2\Pi_{3/2}$	15 979[d]	1.706	954	1.8	16 000	1.720	841
$C\ ^2\Phi_{7/2}$	17 763.50	1.681	977.83	6.53	15 337	1.697	940
$D\ ^2\Pi_{3/2}$	18 009	1.687	878		18 016	1.703	843
$E\ ^2\Pi_{3/2}$	18 104	1.683	995.1	6.9			
$F\ ^2\Phi_{7/2}$	21 151.04	1.6920	938.54	14.03	20 116	1.704	933
$G\ ^2\Phi_{7/2}$	22 309.49	1.6968	938.16[b]				
$H\ ^2\Pi_{3/2}$	23 636.54	1.6665[c]					

[a]From Ref. 16.
[b]This value represents the vibrational interval, $\Delta G_{1/2}$, not ω_e.
[c]This value represents r_0, not r_e.
[d]Vibrational numbering is uncertain in the B-X system. This introduces uncertainty into the parameters ω_e, $\omega_e x_e$, r_e, and especially T_0.

from the $X_1\ ^2\Delta_{5/2}$ level, transitions to the four $^2\Pi_{3/2}$ and three $^2\Phi_{7/2}$ levels are allowed under electric dipole selection rules.

With these facts in hand, it is no surprise that the observed transitions nearly all terminate on upper states with $\Omega' = 3/2$ or 7/2. In fact, it is likely that the four observed upper states with $\Omega' = 3/2$ (the B[16.0] $^2\Pi_{3/2}$, D[18.0] $^2\Pi_{3/2}$, E[18.1] $^2\Pi_{3/2}$, and H[23.6] $^2\Pi_{3/2}$ states) are the four $^2\Pi_{3/2}$ states expected from these excitations. It is also likely that the three observed upper states with $\Omega' = 7/2$ (the C[17.8] $^2\Phi_{7/2}$, F[21.2] $^2\Phi_{7/2}$, and G[22.3] $^2\Phi_{7/2}$ states) are the three expected $^2\Phi_{7/2}$ levels. All of these states are generated by excitation of a nonbonding 1δ or 3σ electron to the antibonding 2π orbital, consistent with the increase in the bond length of 0.05–0.09 Å that is found.

To facilitate a direct comparison to the *ab initio* calculation that was previously reported,[16] Table VIII collects all of the experimentally known information about the electronic states of OsN, which is compared to the previous computational study. It is difficult to directly compare the experimental excitation energies, T_0, with the calculated ones, since the calculation omitted spin-orbit interactions, which are quite significant in this molecule. It is easy to estimate the effects of the spin-orbit operator on the ground $^2\Delta_{5/2}$ level, since this contains only a single hole in an orbital that is nearly purely $5d\delta$ on osmium. Estimating the spin-orbit effects on the excited states is much more difficult, however, since there are multiple $^2\Pi$ and $^2\Phi$ states that derive from the $1\sigma^2\ 2\sigma^2\ 1\pi^4\ 1\delta^3\ 3\sigma^1\ 2\pi^1$ and $1\sigma^2\ 2\sigma^2\ 1\pi^4\ 1\delta^2\ 3\sigma^2\ 2\pi^1$ configurations, and these are strongly mixed by configuration interaction.[16] Thus, disagreements between theory and experiment in the T_0 values could be due to spin-orbit effects. As is commonly found in *ab initio* work on transition metal systems, the calculated bond lengths of the various states are too long, by 0.014 Å on average. The calculated vibrational frequencies tend to be a bit low for the excited electronic states, but the calculated ω_e is in nearly perfect agreement with the measured value for the ground state.

In addition to these $^2\Pi$ and $^2\Phi$ excited states, we also observe one strong band with $\Omega' = 5/2$, which mixes with a nearby dark $\Omega' = 5/2$ state. A fully allowed $\Omega' = 5/2 \leftarrow X\ ^2\Delta_{5/2}$ transition can only occur to another $^2\Delta_{5/2}$ upper state. Thus, there is good evidence of a $^2\Delta_{5/2}$ excited state lying near 22 911.5 cm^{-1}. Such a term cannot arise from promotion of a nonbonding 1δ or 3σ electron to the antibonding 2π orbital. It could arise from promotion of the nonbonding 3σ electron into the strongly antibonding 4σ orbital, leading to a $1\sigma^2\ 2\sigma^2\ 1\pi^4\ 1\delta^3\ 3\sigma^1\ 4\sigma^1$ configuration, or by promotion of a 1π bonding electron into the antibonding 2π orbital, leading to a $1\sigma^2\ 2\sigma^2\ 1\pi^3\ 1\delta^3\ 3\sigma^2\ 2\pi^1$ configuration. Although the energy, bond length, and vibrational frequency were not tabulated, the previous computational study of OsN did report that the $2\ ^2\Delta$ term of OsN derives primarily (69%) from the $1\pi \rightarrow 2\pi$ excitation. Thus, we suspect that the strongly allowed $\Omega' = 5/2 \leftarrow X\ ^2\Delta_{5/2}$ transition near 22 911.5 cm^{-1} is the 0-0 band of this $2\ ^2\Delta_{5/2} \leftarrow X\ ^2\Delta_{5/2}$ transition. Unfortunately, due to strong coupling to the other $\Omega' = 5/2$ level near 22 934 cm^{-1}, it is impossible to provide an accurate estimate of the bond length of this state.

B. Comparison to related molecules

The isoelectronic $5d$ transition metal molecules, ReO,[22,43–46] OsN,[16] and IrC,[25,47–50] have now all been spectroscopically investigated to varying degrees, and have been shown to have a $^2\Delta_{5/2}$ ground state deriving from the $1\sigma^2\ 2\sigma^2\ 1\pi^4\ 1\delta^3\ 3\sigma^2$ configuration. Of these three molecules, the manifold of excited states is now best known for OsN. Although a large number of band systems are known for ReO,[45] our understanding of this molecule is hampered by the fact that the Ω values of the upper states are mostly unknown. An exception is the [14.0]7/2–$X^2\Delta_{5/2}$ band, which has been investigated at 50 MHz resolution, demonstrating that the upper state has an unpaired electron in the 3σ orbital, resulting in a large Fermi contact contribution to the hyperfine splitting.[46] For IrC, upper states in the 14 000–18 000 cm^{-1} range have been reassigned to the $a\ ^4\Phi_{7/2}$, $a\ ^4\Phi_{5/2}$, and $b\ ^4\Pi_{3/2}$ states, all arising from the $1\sigma^2\ 2\sigma^2\ 1\pi^4\ 1\delta^3\ 3\sigma^1\ 2\pi^1$ configuration.[16,48] The analogues of these states are known

in OsN from Fourier transform emission spectroscopy.[16] In addition, three excited states of IrC with $\Omega = 3/2$ and one with $\Omega = 7/2$ have been observed in the 19 000–23 000 cm^{-1} range.[47,49,50] These are undoubtedly analogues of some of the $^2\Pi_{3/2}$ and $^2\Phi_{7/2}$ states observed in OsN in the present study, although it is impossible to draw a precise correlation.

It is also interesting to compare the $5d$, $1\sigma^2\ 2\sigma^2\ 1\pi^4\ 1\delta^3\ 3\sigma^2$, X $^2\Delta_{5/2}$ molecules, ReO, OsN, and IrC, to their isovalent $3d$ and $4d$ counterparts. Both MnO (Ref. 51) and TcO (Ref. 52) have $1\sigma^2\ 2\sigma^2\ 1\pi^4\ 1\delta^2\ 2\pi^2\ 3\sigma^1$, X $^6\Sigma^+$ ground states, while RuN,[53] CoC,[54] and RhC[55] all have $1\sigma^2\ 2\sigma^2\ 1\pi^4\ 1\delta^4\ 3\sigma^1$, X $^2\Sigma^+$ ground states. Only FeN shares the same $1\sigma^2\ 2\sigma^2\ 1\pi^4\ 1\delta^3\ 3\sigma^2$, X $^2\Delta_{5/2}$ ground state that is found in ReO, OsN, and IrC.[56] Hyperfine splitting measurements in CoC, RuN, and RhC show that the 3σ orbital is primarily composed of the transition metal (n+1)s orbital, containing 89% Co $4s$,[54] 63% Ru $5s$,[57] and 70% Rh $5s$ character,[58] respectively. The double occupancy of this 3σ orbital in the $5d$ molecules, ReO, OsN, and IrC, is favored by the relativistic stabilization of the $6s$ orbital in these heavy atoms. Another important factor in the emergence of $1\sigma^2\ 2\sigma^2\ 1\pi^4\ 1\delta^3\ 3\sigma^2$, $^2\Delta_{5/2}$ as the ground state in these $5d$ molecules is the spin-orbit interaction, which stabilizes the $\Omega = 5/2$ component of this state by $-\zeta_{5d}$(M), which amounts to –2545, –3045, and –3617 cm^{-1} in Re, Os, and Ir, respectively.[40] Typically, the magnitude of the spin-orbit stabilization is reduced by a factor of 3 in the $4d$ series, and by a factor of 7 in the $3d$ series,[40] making the spin-orbit stabilization of the $^2\Delta_{5/2}$ level far less significant in the $3d$ and $4d$ series.

The $^6\Sigma^+$ ground states that are found for MnO and TcO are stabilized because the atomic orbitals of the electronegative oxygen atom lie far below those of the metal atom, resulting in significant ionic character and reducing the splitting of the metal nd orbitals. Because the resulting molecular orbitals are little changed from the nd orbitals of the atom, they lie close in energy, favoring the high-spin $^6\Sigma^+$ term. The emergence of the high-spin $^6\Sigma^+$ ground term for highly ionic species is also found for the isovalent transition metal fluoride CrF,[59] and is calculated to be the ground term for MoF and WF as well.[60,61] High spin states are often found for transition metal hydrides for similar reasons: the lack of orbitals of suitable π or δ symmetry on hydrogen prevents the dπ and dδ orbitals from splitting significantly, making it more favorable to place electrons in different orbitals with high-spin coupling, resulting in $^6\Sigma^+$ terms for CrH,[62] MoH,[63] and WH.[64]

V. CONCLUSION

The electronic spectrum of diatomic OsN has been investigated in the range from 19 200 to 23 900 cm^{-1} using resonant two-photon ionization spectroscopy. The study confirms the ground state of OsN to be $^2\Delta_{5/2}$, arising from the $1\sigma^2\ 2\sigma^2\ 1\pi^4\ 1\delta^3\ 3\sigma^2$ electronic configuration. Rotational analysis of 17 bands has revealed four excited states of $^2\Pi_{3/2}$ symmetry and three excited states of $^2\Phi_{7/2}$ symmetry, as expected to arise from the $1\sigma^2\ 2\sigma^2\ 1\pi^4\ 1\delta^3\ 3\sigma^1\ 2\pi^1$ and $1\sigma^2\ 2\sigma^2\ 1\pi^4\ 1\delta^2\ 3\sigma^2\ 2\pi^1$ excited configurations. In addition, one state of $^2\Delta_{5/2}$ symmetry, likely originating from the $1\sigma^2\ 2\sigma^2\ 1\pi^3\ 1\delta^3\ 3\sigma^2\ 2\pi^1$ configuration, has also been found. Spectroscopic constants have been reported and the OsN molecule has been compared to related species.

ACKNOWLEDGMENTS

The authors thank the U.S. Department of Energy for support of this research under Grant No. DE-FG03–01ER15176.

[1] *The Chemical Physics of Solid Surfaces and Heterogeneous Catalyst*. edited by M. Grunze (Elsevier. New York. 1982). Vol. 4.
[2] D. N. Davis. Astrophys. J. **106.** 28 (1949).
[3] H. Spinrad and R. F. Wing. Annu. Rev. Astron. Astrophys. **7.** 269 (1969).
[4] *The Behavior of Chemical Elements in Stars*. edited by C. J. a. M. Jascheck (Cambridge University Press. Cambridge. England. 1995).
[5] R. Yerle. Astron. Astrophys. **73.** 346 (1979).
[6] B. Lindgren and G. Olofsson. Astron. Astrophys. **84.** 300 (1980).
[7] R. S. Ram. P. F. Bernath. and L. Wallace. Astrophys. J.. Suppl. Ser. **107.** 443 (1996).
[8] R. H. Crabtree. *The Organometallic Chemistry of the Transition Metals*. 5th ed. (Wiley. Hoboken. NJ. 2009).
[9] K. E. Andersson. M. Veszelei. and A. Roos. Sol. Energy Mater. Sol. Cells **32.** 199 (1994).
[10] C. G. Ribbing and A. Roos. Proc. SPIE **3133.** 148 (1997).
[11] E. C. Samano. A. Clemente. J. A. Diaz. and G. Soto. Vacuum **85.** 69 (2010).
[12] T. H. Randle. J. Gopalakrishna. and E. D. Doyle. in *Proceedings on Corrosion and Prevention* (2001). pp. 47/1-/8.
[13] F. Levy. P. Hones. P. E. Schmid. R. Sanjines. M. Diserens. and C. Wiemer. Surf. Coat. Technol. **120.** 284 (1999).
[14] P. F. Bernath and S. McLeod. J. Mol. Spectrosc. **207.** 287 (2001).
[15] A. Citra and L. Andrews. J. Phys. Chem. A **104.** 1152 (2000).
[16] R. S. Ram. J. Liévin. and P. F. Bernath. J. Chem. Phys. **111.** 3449 (1999).
[17] W. J. Balfour and R. S. Ram. J. Mol. Spectrosc. **105.** 360 (1984).
[18] O. Krechkivska and M. D. Morse. J. Chem. Phys. **128.** 084314/1 (2008).
[19] R. S. Ram and P. F. Bernath. J. Mol. Spectrosc. **184.** 401 (1997).
[20] R. S. Ram. J. Lievin. and P. F. Bernath. J. Mol. Spectrosc. **215.** 275 (2002).
[21] R. S. Ram and P. F. Bernath. J. Opt. Soc. Am. B **11.** 225 (1994).
[22] W. J. Balfour. J. Cao. C. X. W. Qian. and S. J. Rixon. J. Mol. Spectrosc. **183.** 113 (1997).
[23] R. S. Ram. P. F. Bernath. and W. J. Balfour. J. Mol. Spectrosc. **246.** 192 (2007).
[24] R. S. Ram. J. Liévin. and P. F. Bernath. J. Mol. Spectrosc. **197.** 133 (1999).
[25] A. J. Marr. M. E. Flores. and T. C. Steimle. J. Chem. Phys. **104.** 8183 (1996).
[26] T. C. Steimle. A. J. Marr. S. A. Beaton. and J. M. Brown. J. Chem. Phys. **106.** 2073 (1997).
[27] E. J. Friedman-Hill and R. W. Field. J. Chem. Phys. **100.** 6141 (1994).
[28] T. C. Steimle. K. Y. Jung. and B.-Z. Li. J. Chem. Phys. **103.** 1767 (1995).
[29] D. J. Brugh and M. D. Morse. J. Chem. Phys. **107.** 9772 (1997).
[30] W. C. Wiley and I. H. McLaren. Rev. Sci. Instrum. **26.** 1150 (1955).
[31] B. A. Mamyrin. V. I. Karataev. D. V. Shmikk. and V. A. Zagulin. Zh. Eksp. Teor. Fiz. **64.** 82 (1973).
[32] S. Gerstenkorn and P. Luc. *Atlas du Spectre d'Absorption de la Molécule d'Iode entre 14,800–20,000 cm^{-1}* (CNRS. Paris. 1978).
[33] J. Cariou and P. Luc. *Atlas du Spectre d'Absorption de la Molécule de Tellure entre 18,500–23,800 cm^{-1}* (CNRS. Paris. 1980).
[34] M. D. Morse. in *Methods of Experimental Physics: Atomic, Molecular, and Optical Physics*. Atoms and Molecules Vol. II. edited by F. B. Dunning and R. Hulet (Academic. Orlando. Florida. 1996). pp. 21–47.
[35] S. Gerstenkorn and P. Luc. Rev. Phys. Appl. **14.** 791 (1979).
[36] P. R. Bevington. *Data Reduction and Error Analysis for the Physical Sciences* (McGraw-Hill. New York. 1969).
[37] G. Herzberg. *Molecular Spectra and Molecular Structure I. Spectra of Diatomic Molecules*. 2nd ed. (Van Nostrand Reinhold. New York. 1950).
[38] See supplementary material at http://dx.doi.org/10.1063/1.3633694 for 62 pages of vibronically resolved spectra. isotope shift plots. rotationally resolved spectra. line positions. and rotational fits of OsN.
[39] P. Colarusso. M.-A. Lebeault-Dorget. and B. Simard. Phys. Rev. A **55.** 1526 (1997).
[40] H. Lefebvre-Brion and R. W. Field. *The Spectra and Dynamics of Diatomic Molecules* (Elsevier. Amsterdam. 2004).
[41] J. I. Steinfeld. *Molecules and Radiation: An Introduction to Modern Molecular Spectroscopy*. 2nd ed. (MIT. Cambridge. 1993).

[42]P. F. Bernath, *Spectra of Atoms and Molecules* (Oxford University Press, New York, 1995).
[43]W. J. Balfour and F. B. Orth, J. Mol. Spectrosc. **84**, 424 (1980).
[44]W. J. Balfour and R. S. Ram, J. Mol. Spectrosc. **100**, 164 (1983).
[45]W. J. Balfour and R. S. Ram, Can. J. Phys. **62**, 1524 (1984).
[46]M. A. Roberts, C. G. Alfonzo, K. J. Manke, W. M. Ames, D. B. Ron, and T. D. Varberg, Mol. Phys. **105**, 917 (2007).
[47]K. Jansson, R. Scullman, and B. Yttermo, Chem. Phys. Lett. **4**, 188 (1969).
[48]K. Jansson and R. Scullman, J. Mol. Spectrosc. **36**, 248 (1970).
[49]T. Ma, J. W. H. Leung, and A. S. C. Cheung, Chem. Phys. Lett. **385**, 259 (2004).
[50]H. F. Pang and A. S. C. Cheung, Chem. Phys. Lett. **471**, 194 (2009).
[51]R. M. Gordon and A. J. Merer, Can. J. Phys. **58**, 642 (1980).
[52]S. R. Langhoff, C. W. Bauschlicher,Jr., L. G. M. Pettersson, and P. E. M. Siegbahn, Chem. Phys. **132**, 49 (1989).
[53]R. S. Ram, J. Liévin, and P. F. Bernath, J. Chem. Phys. **109**, 6329 (1998).
[54]M. Barnes, A. J. Merer, and G. F. Metha, J. Chem. Phys. **103**, 8360 (1995).
[55]A. Lagerqvist and R. Scullman, Ark. Fys. **32**, 479 (1966).
[56]K. Aiuchi and K. Shibuya, J. Mol. Spectrosc. **204**, 235 (2000).
[57]T. C. Steimle and W. Virgo, J. Chem. Phys. **119**, 12965 (2003).
[58]J. M. Brom, Jr., W. R. M. Graham, and W. Weltner,Jr., J. Chem. Phys. **57**, 4116 (1972).
[59]O. Launila, J. Mol. Spectrosc. **169**, 373 (1995).
[60]L. Cheng, M. Y. Wang, Z. J. Wu, and Z. M. Su, J. Comput. Chem. **28**, 2190 (2007).
[61]K. G. Dyall, J. Phys. Chem. A **104**, 4077 (2000).
[62]R. S. Ram, C. N. Jarman, and P. F. Bernath, J. Mol. Spectrosc. **161**, 445 (1993).
[63]K. Balasubramanian and J. Li, J. Phys. Chem. **94**, 4415 (1990).
[64]Z. Ma and K. Balasubramanian, Chem. Phys. Lett. **181**, 467 (1991).